AIAA JOURNAL
Vol. 47, No. 4, April 2009

Technical Notes

TECHNICAL NOTES are short manuscripts describing new developments or important results of a preliminary nature. These Notes should not exceed 2500 words (where a figure or table counts as 200 words). Following informal review by the Editors, they may be published within a few months of the date of receipt. Style requirements are the same as for regular contributions (see inside back cover).

Side Force Suppression by Dimples on Ogive-Cylinder Body

Y. D. Cui* and H. M. Tsai†
National University of Singapore, Singapore 117508, Republic of Singapore

DOI: 10.2514/1.39176

Nomenclature

Cp	=	pressure coefficient, $(P - P_\infty)/q$
Cy	=	side force coefficient, $F_Y/(qS)$
D	=	base diameter of cylinder
F_Y	=	side force
h	=	dimple depth
L	=	distance between two rows of dimples
P	=	surface pressure
P_∞	=	freestream static pressure
q	=	dynamic pressure, $0.5\rho U^2$
R	=	radius of cylinder
Re	=	Reynolds number, UD/ν
r	=	radius of cutting sphere to form dimple
S	=	model base area, $\pi D^2/4$
U	=	freestream velocity
α	=	angle of attack
θ	=	azimuthal angle around cylinder cross section measured from the most leeward position
ν	=	kinematic viscosity of fluid
ρ	=	density of fluid
φ	=	roll angle

I. Introduction

IT IS known that the vortex pair formed over the leeward side of symmetric slender bodies becomes asymmetric when the angle of attack is beyond a critical value, leading to undesirable large side forces [1]. The proposed explanation of this phenomenon varies from hydrodynamic instability hypothesis (including convective and/or absolute-type instability) to asymmetric flow separation and/or reattachment [1–4]. Over the years the needs for suppressing the formation of side forces have led many researchers to propose different flow control techniques and devices [5,6], such as strakes, blowing and suction, boundary-layer trips, surface roughening, and rounding of the ogive nose tip. The search for effective and robust means in reducing the large side force is ongoing.

The use of dimples for flow control over a flat plate, circular cylinder, or sphere has been reported [7–9]. In the present study, the effectiveness of dimples in suppressing the large side forces over an ogival cylinder body at high angles of attack was examined. To this end, force and surface pressure measurements in a wind tunnel are made to assess their effectiveness, combined with flow visualizations in a water tunnel to provide further insight of the flow caused by the dimples.

II. Experimental Details

The experiments were made in the low speed wind-tunnel (0.45×0.45 m test section) and water tunnel (1.0×0.75 m test section) at Temasek Laboratories of the National University of Singapore. Figure 1 shows the test rig used for the wind-tunnel tests. The measurements were made at a freestream velocity of about 11.3 ± 0.1 m/s with a freestream turbulent intensity less than 0.4%, corresponding to a Reynolds number of 2.6×10^4. For the experiment, the model protrudes through a hole on the bottom wall of the wind-tunnel test section (not shown in the figure). The sting (shaft) of the model is connected to a stepper motor to provide roll movement. Both the model and the stepper motor are fixed on an inclined angle mechanism, through which the angles of attack can be adjusted by the predetermined pin holes on it, with an accuracy of about 0.5 deg. The entire mechanism is then mounted on a 6-degree-of-freedom force balance (load cell), which in turn is connected to a rotation gauge with resolution of $1/60$ deg to adjust accurately the side-slip angle. For force measurements, the factory calibration data were used. However, the side force component was consistently checked, showing the balance had uncertainty of less than 5% of the locally measured value and drifted about 10% of the locally measured value. We note that the impact of 10% drift on the measurements is minimal and in no way affects the trend of the measurements for different angles of attack. For water tunnel experiments, a similar setup was used except that it was set upside down to avoid interferences from the free surface and for ease of capturing flow images through the bottom window.

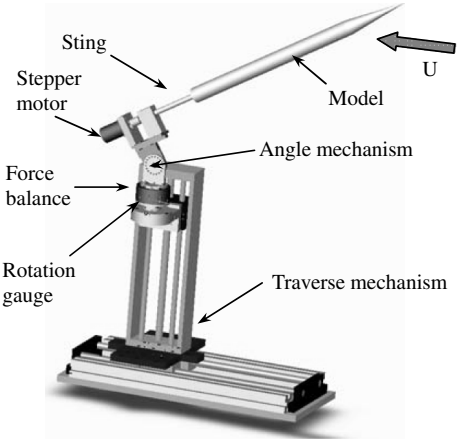

Fig. 1 Schematic of the experimental setup for the wind tunnel used.

Presented as Paper 2008-0368 at the 46th AIAA Aerospace Sciences Meeting and Exhibit, Grand Sierra Resort Hotel, Reno, Nevada, 7–10 January 2008; received 17 June 2008; revision received 29 December 2008; accepted for publication 13 January 2009.

*Research Scientist, Temasek Laboratories, 5 Sports Drive 2. Member AIAA.

†Currently at Singapore Science Centre, Singapore 609081, Republic of Singapore.

For the present study, dimples are applied only to the front part of the ogive-cylinder model because the apex region has the most influence in controlling the flow. A smooth ogive-cylinder model (model A) with a nose length of 3.5D (122.5 mm) and a total body length of 16D (560 mm) was used as the baseline. Model B is identical except for the dimpled surface applied to the front portion (190 mm in length) as shown in Fig. 2. Both models were made using a rapid prototyping technique (Objet FullCure 700 resin) with a stated maximum tolerance of about 0.1 mm. Only one dimple arrangement is studied here. The dimples are formed with sharp edges by "sphere cutting" with the CAD program. The first row of dimples starts on the cylinder part at 4.7D (164 mm) from the tip of the model. Eight equally spaced dimples were formed around the circumference of the cylinder, and the same pattern is repeated with a spacing (L), but in a staggered manner. Because on the ogive nose, the local radius is not constant, the radius of the cutting sphere (r) and the depth of dimple (h) are linearly scaled by the ratio of the local radius of the ogive nose part to the cylinder radius (R). L is determined by keeping the density of dimples (ratio of dimples area to total surface area of the two rows, about 25.6%) constant. An iterative process is needed to determine L. Hence both dimple depth and diameter are functions of the local diameter of the nose.

To measure the pressure distribution, three rows of equally spaced pressure tapping holes are located at 80 mm (station 1), 140 mm (station 2), and 210 mm (station 3) from the tip of the models, with eight pressure tapping holes at the first station, and 16 tapping holes at the other two stations. Note that stations 1 and 2 are located in the region between two rows of dimples whereas station 3 is located on the smooth cylinder part. The pressure measurements were made using a unidirectional differential pressure transducer with a measurement range of 0 to 1 in. of water with an accuracy of $\pm 0.14\%$ of the full scale, which translates into a maximum error of ± 0.005 for the pressure coefficient at a freestream wind speed of 11.3 m/s. Voltage data from the transducer were acquired using a National Instrument data acquisition card at a sampling frequency of 100 Hz over a period of 60 s.

III. Results and Discussions

Figure 3 shows the side force coefficient variation with roll angle at various angles of attack for models A and B. It can be seen that the side force for model A is small at $\alpha = 25$ deg, but larger at $\alpha = 30$ deg. As α increase to 40 and 50 deg, the pattern of the side force with the roll angle shows an abrupt switchover between the positive and negative, indicating the existence of bistable states. The overall force and pressure measurements for model A are consistent with those of other studies [10,11]. For model B with dimpled surface, the side force is significantly reduced even at $\alpha = 40$ deg. At $\alpha = 50$ deg, the side force shows values comparable to those without dimples but with a higher level of fluctuations. The fluctuations observed at all angles of attack are randomlike but show some correlations with the orientation of the dimples. A point where the side force is small is also present unlike the distinct bistable state of model A at $\alpha = 50$ deg. It is clear that dimples, although suppressing the side forces at high angles of attack, also introduce fluctuations albeit of a smaller magnitude at low angles of attack.

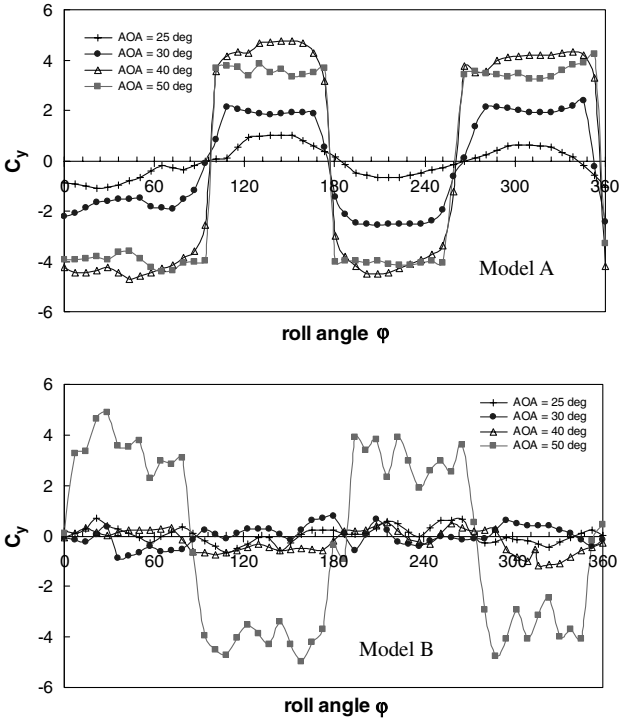

Fig. 3 Side force coefficient variation with roll angle for models A and B at various angles of attack with $Re = 2.6 \times 10^4$.

To further investigate the influence of the dimples, surface static pressures were measured. At the Reynolds numbers of the experiment, it is known that the boundary layer on a smooth ogive-cylinder body is in the laminar regime [10]. Note that the overall pressure distributions for model A show the laminar separation behavior with little pressure recovery (see model A in Fig. 4), which are consistent with those of Luo et al. [11]. For brevity, only typical pressure distributions for models A and B at $\alpha = 40$ deg are shown in Fig. 4. For model B, it can be seen that the pressure distribution is asymmetric for the three roll angles, and larger pressure recovery with a more leeward separation location compared to model A at station 2, indicating the flow to be turbulent. The pressure distribution changes with roll angles are also notable, which is due to the fact that the dimple layout with respect to the azimuthal angle is different when the model is at different roll angles. Though the

Table 1. Dimensions of dimples on cylinder part

D (mm)	R (mm)	r (mm)	h (mm)	L (mm)
35	17.5	8.785	1.417	17

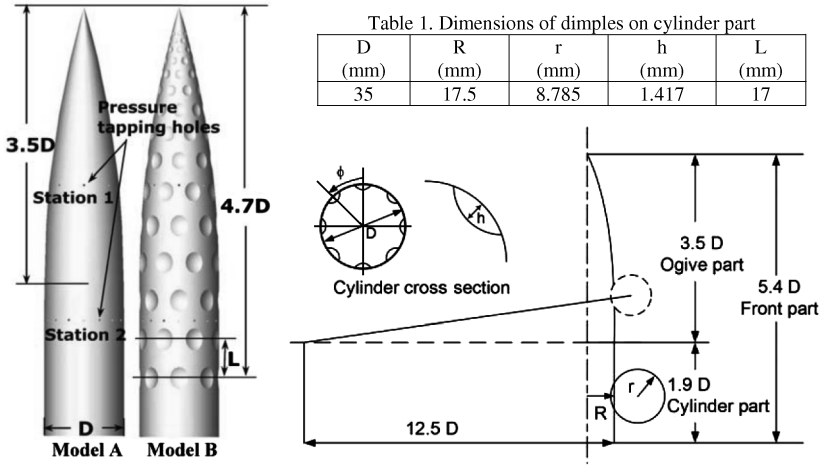

Fig. 2 Drawings of the front parts of models and sketch of dimples formation.

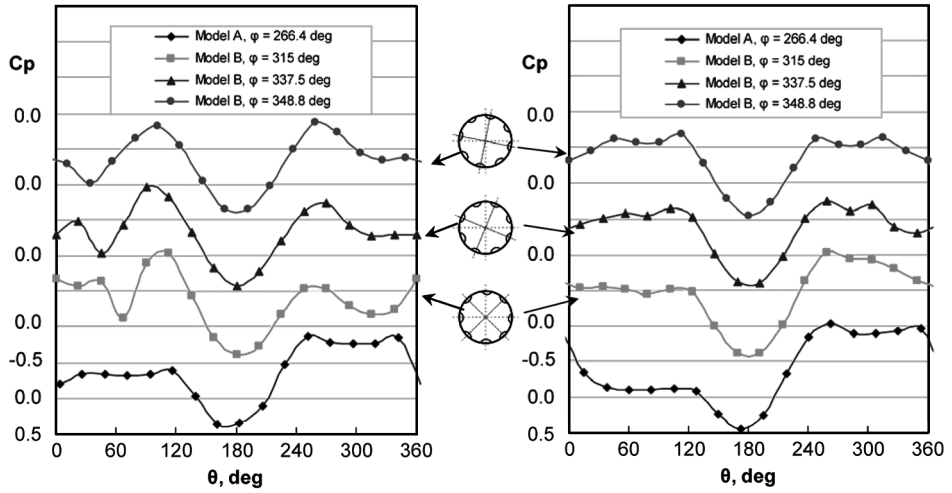

a) Station 2 b) Station 3

Fig. 4 Pressure coefficient variation with azimuthal angle θ at $\alpha = 40$ deg, and roll angles as indicated for models A and B at stations 2 and 3 with $Re = 2.6 \times 10^4$.

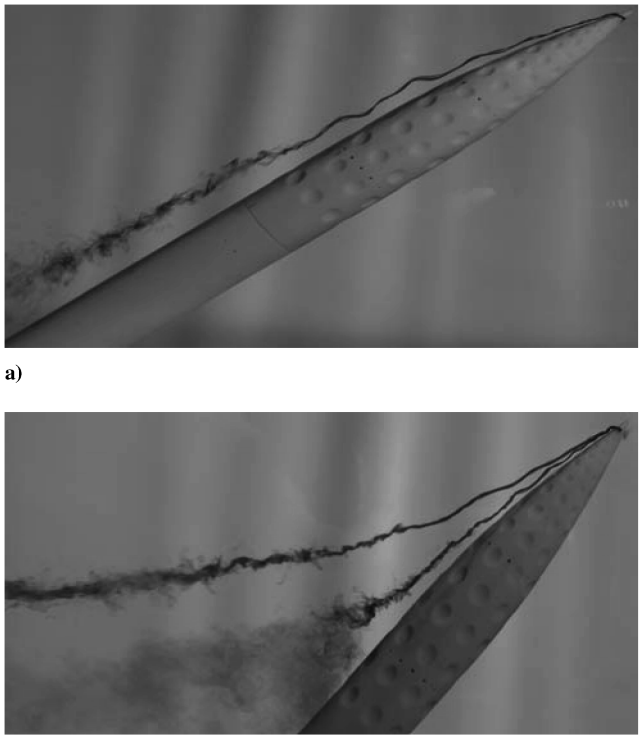

a)

b)

Fig. 5 Flow visualization images at a) $\alpha = 40$ deg and b) $\alpha = 50$ deg for model B at $Re = 6 \times 10^3$.

pressure distribution for model B is not symmetric, the measured side forces are small, in contrast for the smooth ogive which shows complete asymmetric pressure distribution and large side forces. These results show that the existence of dimples on the front portion of the ogive-cylinder model modifies the flowfield leading to reduced side force at high angles of attack.

To further understand how dimples affect the flow around the body, flow visualization using dye for model B was made in the water tunnel. In the interest of producing clearer flow features, most of the visualizations were at $Re = 6000$ which is 4 times smaller that the wind-tunnel experiments discussed previously. It is noted here that flow visualizations were also attempted at a Reynolds number about of 20,000, with the overall pattern and flow features being similar to those at the lower Reynolds number of 6000. But as is evident, the images are less distinct due to the greater diffusion of the dye at higher Reynolds numbers (not shown here).

Figure 5 shows the side views of flow visualization images at $\alpha = 40$ deg and 50 deg. It can be seen that at $\alpha = 40$ deg the vortices appear to be symmetric at the front part of the model and become unsteady downstream of the model. This is clear from the diffusion of dye filament in that the vortex core seems to become turbulent. Note that the trajectory of dye (vortex core) is also influenced by the presence of the dimples on the surface in a meandering manner. It is also observed that at $\alpha = 40$ deg the flow structures for different roll angles are almost the same. However when $\alpha = 50$ deg, the vortex asymmetry is obvious, indicating the side forces are related with the flow state (symmetric or asymmetric vortices).

To further obtain clues about the effects of dimples, some dye was injected into the flowfield through the pressure taping holes as shown in Fig. 6. This method is not altogether satisfactory to view detail

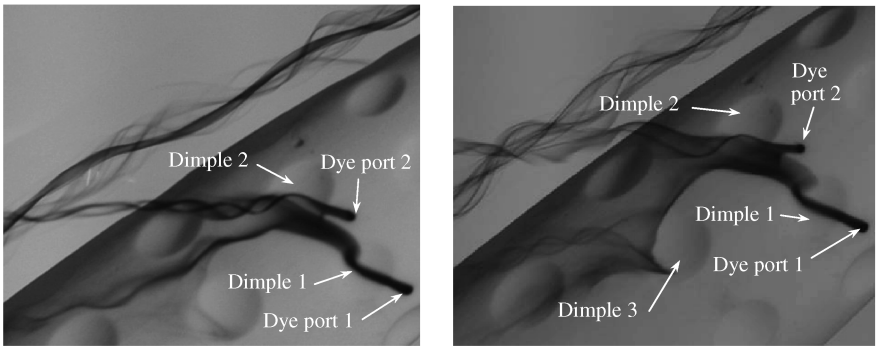

a) $\alpha = 40^o$, $\varphi = 43.2^o$ b) $\alpha = 40^o$, $\varphi = 50.4^o$

Fig. 6 Flow visualization around dimples at $\alpha = 40$ deg at two different roll angles for model B at $Re = 6 \times 10^3$.

flow structures but nonetheless offers us some insight of the flow. At $\phi = 43.2$ deg, Fig. 6a shows that the flow (dye) from dye port 1, entering the nearby dimple (dimple 1) almost at its center, flows toward to the leeward side, and then turns around at the edge of dimple 2. The dye from dye port 2 drifts downstream via dimple 2 and is ejected out of the dimple showing a helical flow path before it wraps around the main primary vortex. With a small roll to $\phi = 50.4$ deg, unlike the case of $\phi = 43.2$ deg, the dye from dye port 1 now is sucked into dimple 3 after turning around near dimple 2, where it is then ejected periodically. Also, the dye from port 2 passes through dimple 2 and is ejected intermittently to form a vortexlike structure downstream. The video clearly shows that the dye (flow) is brought into the dimple and subsequently ejected in an intermittent manner forming a small vortex structure. With different roll orientation of the cylinder, similar flow behavior around the dimple can be examined.

IV. Conclusions

Experiments carried out on a dimpled ogive-cylinder body show that the side force can be reduced at high angles of attack up to 40 deg with a symmetric vortex pair over the leeward side. The use of dimples in reducing larger side forces is robust and is not sensitive to the roll angle. From the force and pressure measurements as well as flow visualization, the following observations are highlighted: 1) the vortex flow is still the dominant feature, that is, the dimpled surface does not destroy the coherence of the primary vortex pair; 2) dimples trigger turbulent boundary-layer transition, and cause a more leeward turbulent separation, leading to changes in local pressure distribution; and 3) the flow tends to be intermittently separated from the dimple to form turbulent structures or the formation of small vortical structures of the scale of the dimples, which in turn interacts and modulates the primary flowfield.

No attempts were made here to optimize the dimple dimensions and layout. Studies are needed to further understand the mechanism of a dimpled surface in suppressing side forces, and to map the regimes where dimple depths and arrangements can more effectively control the side force. Further studies are also needed to examine if the effects of dimples on the side forces are sensitive to Reynolds numbers.

Acknowledgment

The authors gratefully acknowledge the support from the Directorate of Research and Development, Defense Science and Technology Agency, Singapore, under the Flow Control Program POD-0103935.

References

[1] Champigny, P., "Side Forces at High Angles of Attack; Why, When, How?," *La Recherche Aerospatiale*, No. 4, 1994, pp. 269–282.

[2] Degani, D., "Instabilities of Flows Over Bodies at Large Incidence," *AIAA Journal*, Vol. 30, No. 1, 1992, pp. 94–100. doi:10.2514/3.10887

[3] Ericsson, L., and Reding, J., "Asymmetric Flow Separation and Vortex Shedding on Bodies of Revolution," *Tactical Missile Aerodynamics: General Topics*, edited by M. Hemsh, Vol. 141, Progress in Astronautics and Aeronautics, AIAA, New York, 1992, pp. 391–452.

[4] Cummings, R., Forsythe, J., Morton, S., and Squires, K., "Computational Challenges in High Angle of Attack Flow Prediction," *Progress in Aerospace Sciences*, Vol. 39, No. 5, 2003, pp. 369–384. doi:10.1016/S0376-0421(03)00041-1

[5] Malcolm, G. N., "Forebody Vortex Control," *Progress in Aerospace Sciences*, Vol. 28, No. 3, 1991, pp. 171–234. doi:10.1016/0376-0421(91)90005-O

[6] Williams, D., "A Review of Forebody Vortex Control Scenarios," AIAA Paper 97-1967, 1997.

[7] Bearman, P. W., and Harvey, J. K., "Control of Circular Cylinder Flow by the Use of Dimples," *AIAA Journal*, Vol. 31, No. 10, 1993, pp. 1753–1756. doi:10.2514/3.11844

[8] Won, S. Y., Zhang, Q., and Ligrani, P. M., "Comparisons of Flow Structure Above Dimpled Surfaces with Different Dimple Depths in a Channel," *Physics of Fluids*, Vol. 17, No. 4, 2005, p. 045105. doi:10.1063/1.1872073

[9] Choi, J., Jeon, W. P., and Choi, H., "Mechanism of Drag Reduction by Dimples on a Sphere," *Physics of Fluids*, Vol. 18, No. 4, 2006, p. 041702. doi:10.1063/1.2191848

[10] Lamont, P. J., "Pressure Around an Inclined Ogive Cylinder with Laminar, Transitional, or Turbulent Separation," *AIAA Journal*, Vol. 20, No. 11, 1982, pp. 1492–1499. doi:10.2514/3.51212

[11] Luo, S. C., Lim, T. T., Lua, K. B., Chia, H. T., Goh, E. K. R., and Ho, Q. W., "Flowfield Around Ogive/Elliptic-Tip Cylinder at High Angle of Attack," *AIAA Journal*, Vol. 36, No. 10, Oct. 1998, pp. 1778–1787. doi:10.2514/2.286

J. Samareh
Associate Editor